

AirCargoChallenge 2022

Technical Report

Team #29

WUT AeroDesign



SAE

AeroDesign

Table of Contents

| | |
|---|----|
| Table of figures..... | 4 |
| Table of tables..... | 4 |
| Table of acronyms..... | 5 |
| Table of appendixes..... | 5 |
| 1. Introduction..... | 6 |
| 2. Discriminators..... | 6 |
| 3. Project management..... | 7 |
| 3.1. Structure of the organization..... | 7 |
| 3.2. Finance and budget..... | 7 |
| 3.3. Time line..... | 8 |
| 4. Propeller selection..... | 9 |
| 5. Initial design..... | 10 |
| 5.1. Design assumptions..... | 10 |
| 5.2. Initial calculations..... | 11 |
| 5.3. Payload prediction..... | 11 |
| 6. Aerodynamic design..... | 12 |
| 6.1. Airfoil selection..... | 12 |
| 6.2. Wing design..... | 13 |
| 6.3. Winglet design..... | 14 |
| 6.4. Stabilator design..... | 14 |
| 6.5. Fin design..... | 15 |
| 6.6. Servo sizing..... | 15 |
| 6.7. Plane polars..... | 15 |
| 7. Stability and control..... | 16 |
| 7.1. Mass analysis..... | 16 |
| 7.2. Static stability..... | 16 |
| 7.3. Dynamic stability..... | 18 |
| 8. Structural design..... | 18 |
| 8.1. Flight envelope..... | 18 |
| 8.2. Wing..... | 19 |
| 8.3. Winglets..... | 20 |
| 8.4. Stabilator..... | 20 |
| 8.5. Fin..... | 20 |
| 8.6. Fuselage and cargo bay..... | 21 |
| 8.7. Tail boom..... | 21 |

| | | |
|------|---------------------------------------|----|
| 8.8. | Landing gear | 22 |
| 8.9. | Structural division..... | 22 |
| 9. | Performance..... | 23 |
| 9.1. | Climb rate and horizontal speed | 23 |
| 9.2. | Turn analysis..... | 24 |
| 9.3. | Take-off run analysis | 25 |
| 9.4. | Representative properties..... | 26 |
| 10. | Outlook..... | 26 |

Table of figures

| | | |
|-----------|--|----|
| Figure 1 | Render of Mosquito's assembly | 6 |
| Figure 2 | Discriminators..... | 7 |
| Figure 3 | Summary of the financial expenses..... | 8 |
| Figure 4 | Project's time line | 8 |
| Figure 5 | Thrust of examined propellers | 9 |
| Figure 6 | Wind tunnel test station..... | 9 |
| Figure 7 | Propeller's mounting on the motor..... | 10 |
| Figure 8 | Payload prediction curve..... | 12 |
| Figure 9 | Chosen airfoils | 12 |
| Figure 10 | Airfoil polars | 13 |
| Figure 11 | Wing twist..... | 13 |
| Figure 12 | Winglets impact on the induced drag of the wing | 14 |
| Figure 13 | Plane shape inside of the rhombus box | 15 |
| Figure 14 | Plane polars | 16 |
| Figure 15 | Neutral points of stability (blue) and maneuverability (orange) chart | 17 |
| Figure 16 | Margins of stability (blue) and maneuverability (orange) chart | 17 |
| Figure 17 | Flight envelope | 18 |
| Figure 18 | Wing loads chart..... | 19 |
| Figure 19 | Mounting rib molder with gumosil negative..... | 19 |
| Figure 20 | Wing spar with molder | 20 |
| Figure 21 | Fuselage design | 21 |
| Figure 22 | Cargo bay accommodations | 21 |
| Figure 23 | Tail boom displacement chart and measurement method..... | 22 |
| Figure 24 | Landing gear test platform | 22 |
| Figure 25 | Aircraft structural division..... | 23 |
| Figure 26 | Climb rate chart..... | 24 |
| Figure 27 | Turn radius analysis with the cruise speed VC (blue dotted line) and smallest diameter of the airfield (dark green dotted line)..... | 25 |
| Figure 28 | Take-off length chart | 25 |

Table of tables

| | | |
|---------|--|----|
| Table 1 | Brief comparison of wing configurations..... | 10 |
|---------|--|----|

| | |
|------------------------------------|----|
| Table 2 Servo sizing | 15 |
| Table 3 Mass analysis | 16 |
| Table 4 Damping coefficients | 18 |
| Table 5 Performance summary | 26 |

Table of acronyms

ACC – Air Cargo Challenge
 AoA – angle of attack
 Cd – drag coefficient
 CG – Center of gravity
 Cl – lift coefficient
 Cm – pitching moment coefficient
 WUT- Warsaw University of Technology

Table of appendixes

Appendix 1: 3-view drawing of the aircraft
 Appendix 2: Isometric perspective view of the aircraft
 Appendix 3: Cargo bay, AME, RX location
 Appendix 4: Mounting of the wing to the fuselage

1. Introduction

WUT SAE Aero Design Collegiate Club would like to present its Air Cargo class aircraft for the Air Cargo Challenge 2022 –“Mosquito”. According to the competition regulations, the plane is adapted to transport blood, which is enabled by a specially designed Cargo compartment. Our team has created a plane with a curb weight of 2,4 kg and able to carry a load of 3,2 kg. The main assumption of the project was to create an aircraft capable of short take-off and landing from a grass runway, and at the same time able to develop high speed and carry a large load.

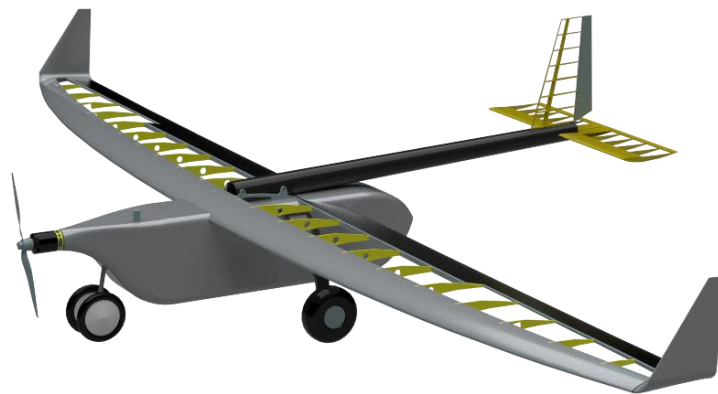


Figure 1 Render of Mosquito's assembly

2. Discriminators

The most characteristic feature of the aircraft is high volume fuselage with access to cargo bay from one of the sides. To provide low traction on grass airstrip and high stability on potholes the main landing gear has wide spacing and nose landing gear consists of two wheels. To improve Cl^3/Cd^2 characteristics the winglets were designed.

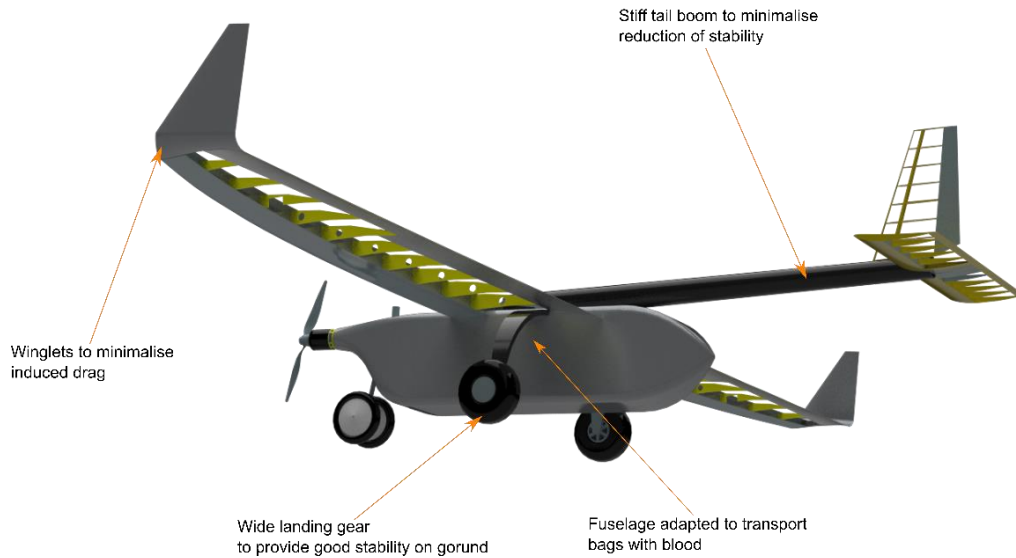


Figure 2 Discriminators

3. Project management

This chapter contains information on the topic of team's and organization's management, financing and project's advancements through time.

3.1. Structure of the organization

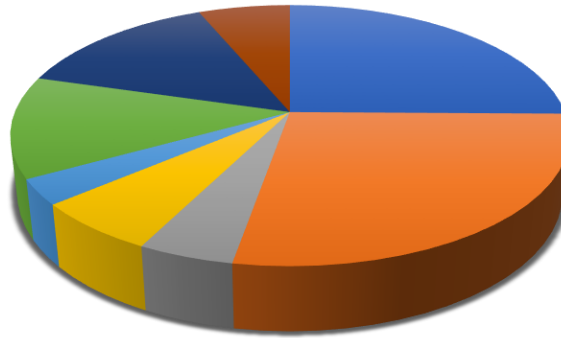
Our Association has a very defined organizational structure, the management board is responsible for the entirety of the work as well as financial and administrative matters. We carry out many projects every year, and coordinators are responsible for each of them, they are also the main people designing a given plane and coordinating all the works. The coordinators have a group of people at their disposal who help them in the design, calculation and testing process on an ongoing basis. The construction of the aircraft is carried out by the entire team of our association, supervised by the main coordinator and his team. This management structure has been developed over the years and allows us to achieve high places in international competitions.

3.2. Finance and budget

Our association has very large technological resources, which means that we are able to do most of the work ourselves, using our technical background. Therefore, the main cost of making an aircraft is the purchase of materials.

The main source of funding is the government project "Student Associations create innovation" which allows us to purchase the necessary materials. Our association has many sponsors who finance the construction of our plane and participation in competitions. The authorities of our university also finance our projects.

Total Costs



- Car rental + fuel - 1600€
- Administration Costs - 1750€
- Fabrics - 300€
- Construction Materials - 400€
- Batteries - 200€
- Electronics - 800€
- CNC milling - 900€
- Prolab plates - 400€

Figure 3 Summary of the financial expenses

3.3. Time line

We started works on the conceptual design of the plane in September 2021. Practically from the beginning of the project development, part of our group was involved in the valuation of the project and obtaining funds, including acquiring sponsors. The construction of the plane started with a considerable delay, which was caused by a lack of funds for the purchase of materials. In the near future, we are determined to finish construction of the first prototype in order to take it for first flight tests.

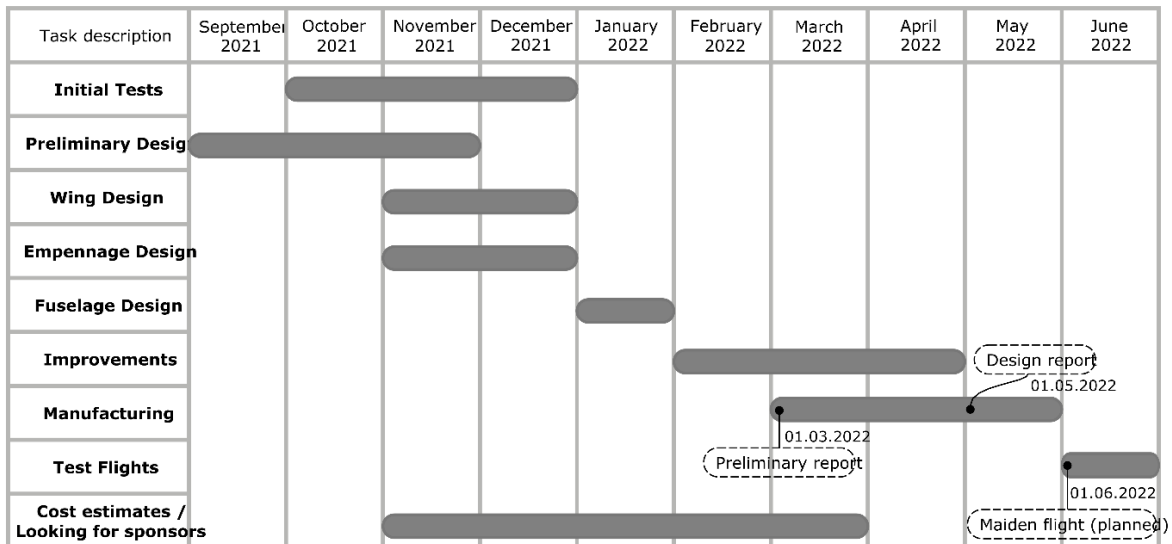


Figure 4 Project's time line

4. Propeller selection

The competition regulations strictly define motor and propeller models that can be used in designed airplanes, therefore appropriate tests were priority to determine available thrust. On its basis, it was possible to define further design assumptions, described in more detail in the next section. The purchased motor and propellers were tested in a wind tunnel for various air flow speeds simulating different flight conditions. Both static and dynamic tests were performed according to the voltage limits described in the regulations. The obtained values were read from our custom made test bench and the results are as follows:

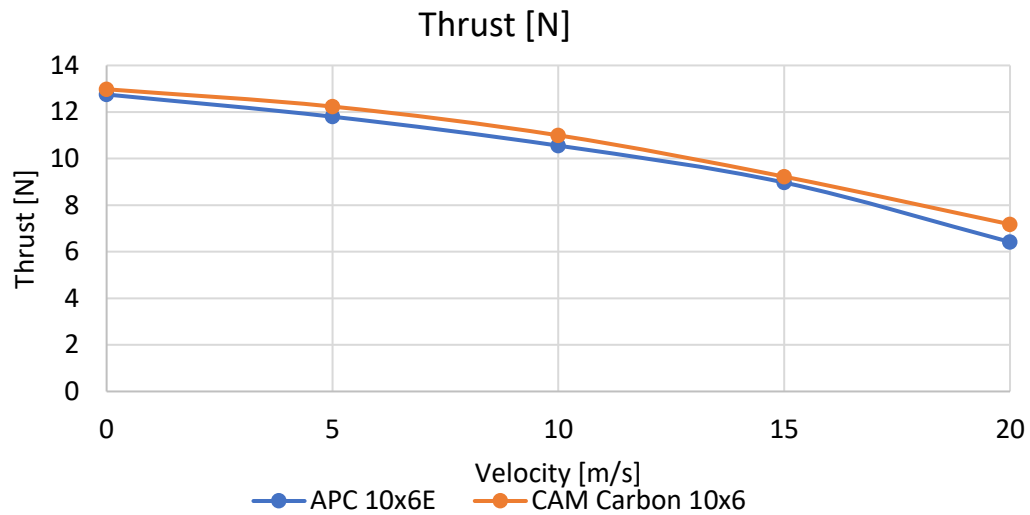


Figure 5 Thrust of examined propellers

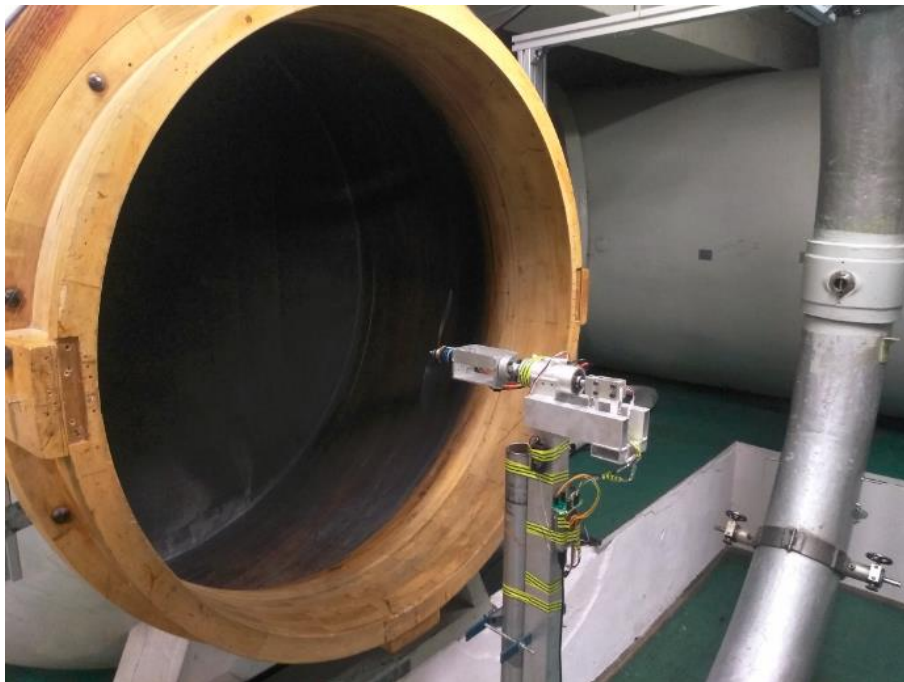


Figure 6 Wind tunnel test station



Figure 7 Propeller's mounting on the motor

5. Initial design

This chapter contains information on the topic of initial assumptions and scoring predictions of the aircraft.

5.1. Design assumptions

During the initial design there were considered three different configurations: classical low wing, classical high wing and flying wing configuration. Advantages and disadvantages of each configuration are presented in Table 1.

Table 1 Brief comparison of wing configurations

| Wing configuration | Advantages | Disadvantages |
|--------------------|--|--|
| Low wing | <ul style="list-style-type: none"> - Short landing gear - Shortest take-off due to the presence of ground effect - Good access to the cargo bay | <ul style="list-style-type: none"> - Medium vertical and lateral stability |
| High wing | <ul style="list-style-type: none"> - Good vertical and lateral stability - Landing gear easy to design | <ul style="list-style-type: none"> - Poor access to the cargo bay - Long landing gear struts |
| Flying wing | <ul style="list-style-type: none"> - Lowest drag - Very good access to the cargo bay | <ul style="list-style-type: none"> - Poor lateral and vertical stability - High momentum of inertia due to thick airfoils - Prohibited artificial stability |

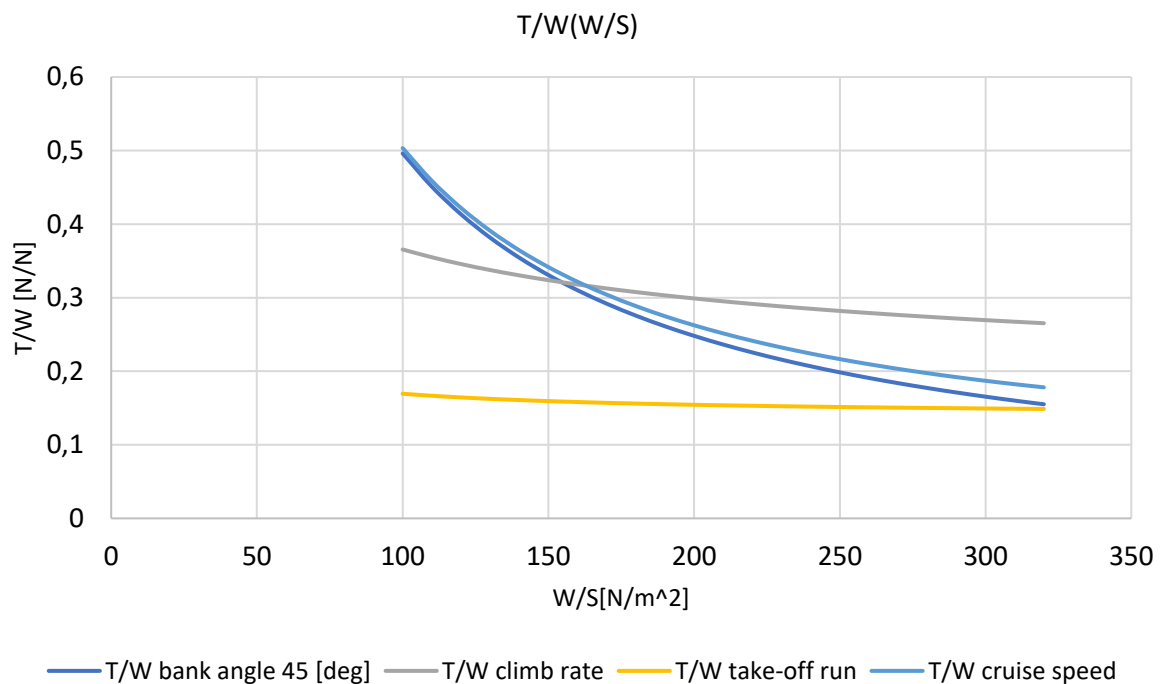
The team decided to use high wing configuration due to its high stability and fact that payload mass is almost equal to empty mass of the aircraft.

The idea was to design high wing aircraft with light weight fuselage. In order to minimize mass of the structure the team designed landing gear and tail boom mounted to the wing. Empennage was planned classic to prevent flow separation in condition of deep stall.

Also due to sizing limitations it was concluded that appliance of flaps will excessively increase pitching moment which could be very hard to compensate with small horizontal stabilizer.

At this point team decided to design aircraft capable of reaching climb rate of 1,8 m/s and maximizing mass of the cargo. The selection of the runway length was neglected at this point.

The thrust/weight weight/wing area plot was used to establish assumptions of the main properties of the aircraft.



5.2. Initial calculations

After measuring the disposable thrust, a scoring strategy was developed. The team assumed that climb rate and payload mass would be most beneficial and easiest to achieve, as they require common properties to be maximized. The maximum speed and loading/unloading time were of secondary importance. Therefore, a score computation algorithm in MATLAB software was created. It helped us to obtain optimal parameters which should provide the best possible performance in terms of maximum climb rate and payload mass. All in all our aircraft will be able to climb with $w=1,8$ m/s and carry $m=3,2$ kg of payload.

5.3. Payload prediction

The payload prediction curve was computed for final configuration. Changes in dynamic pressure and thrust were considered. The payload prediction curve and formula are presented below.

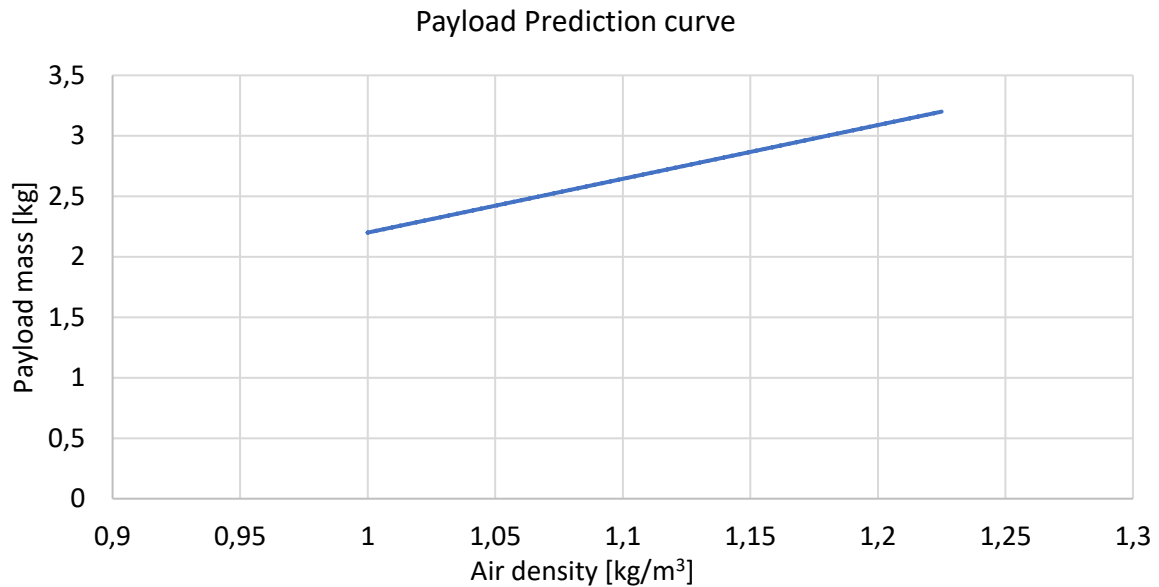


Figure 8 Payload prediction curve

$$\text{Payload mass [kg]} = 4,44 * \text{Air density} \left[\frac{\text{kg}}{\text{m}^3} \right] - 2,24$$

6. Aerodynamic design

This chapter contains information on the topic of aerodynamic properties of the plane, airfoil selection and design assumptions for the main wing and empennage. During the design process the team used AVL and XFLR5 software along with analytical formulas.

6.1. Airfoil selection

During the initial design the Reynolds number was calculated approximately to 250 000. There were 3 airfoils considered (Selig 3024, Selig 4320 and PP02) to make reference.

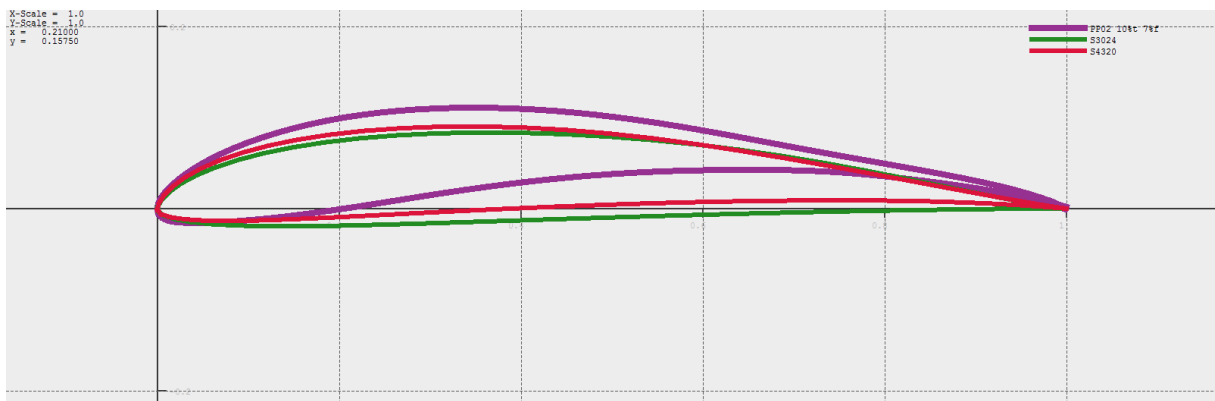


Figure 9 Chosen airfoils

The airfoil chosen for the main wing is PP02 with 10% thickness and 7% camber. The airfoil is based on Selig airfoil series. Selected airfoil has high Cl^3/Cd^2 and slightly larger drag at low angles of attack (Fig. 10).

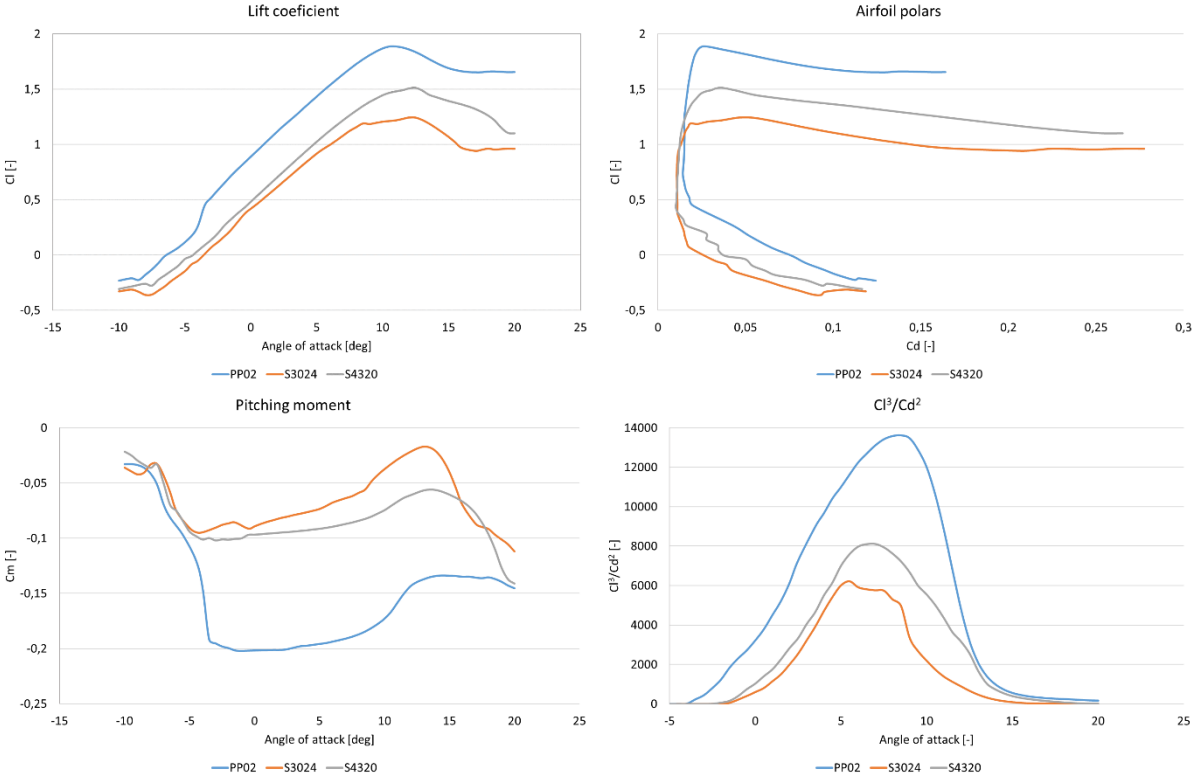


Figure 10 Airfoil polars

6.2. Wing design

A decision was made to design elliptical wing with a straight trailing edge to minimize 3D airflow behind the wing. According to the Munk law, an elliptical wing provides elliptical load distribution which has the smallest induced drag. The negative aspect of this configuration is bad stall characteristics (flow separation occurs at the half of trailing edge) caused by rectangular Cl distribution. To improve stall characteristics geometrical wing twist was used.

Twist of the wing

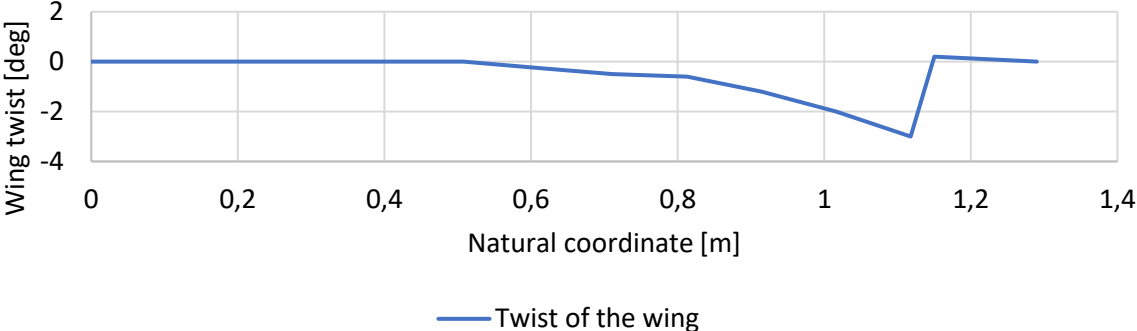


Figure 11Wing twist

6.3. Winglet design

Aiming to decrease induced drag it was decided to design winglets. The aim was to obtain proportional distribution of induced angle to cosine of the angle of lateral inclination. It was achieved through the usage of twist and both Selig 3010 and Selig 9032 airfoils. Presence of winglets decreased induced drag by 10% and increased Cl^3/Cd^2 ratio about 15%.

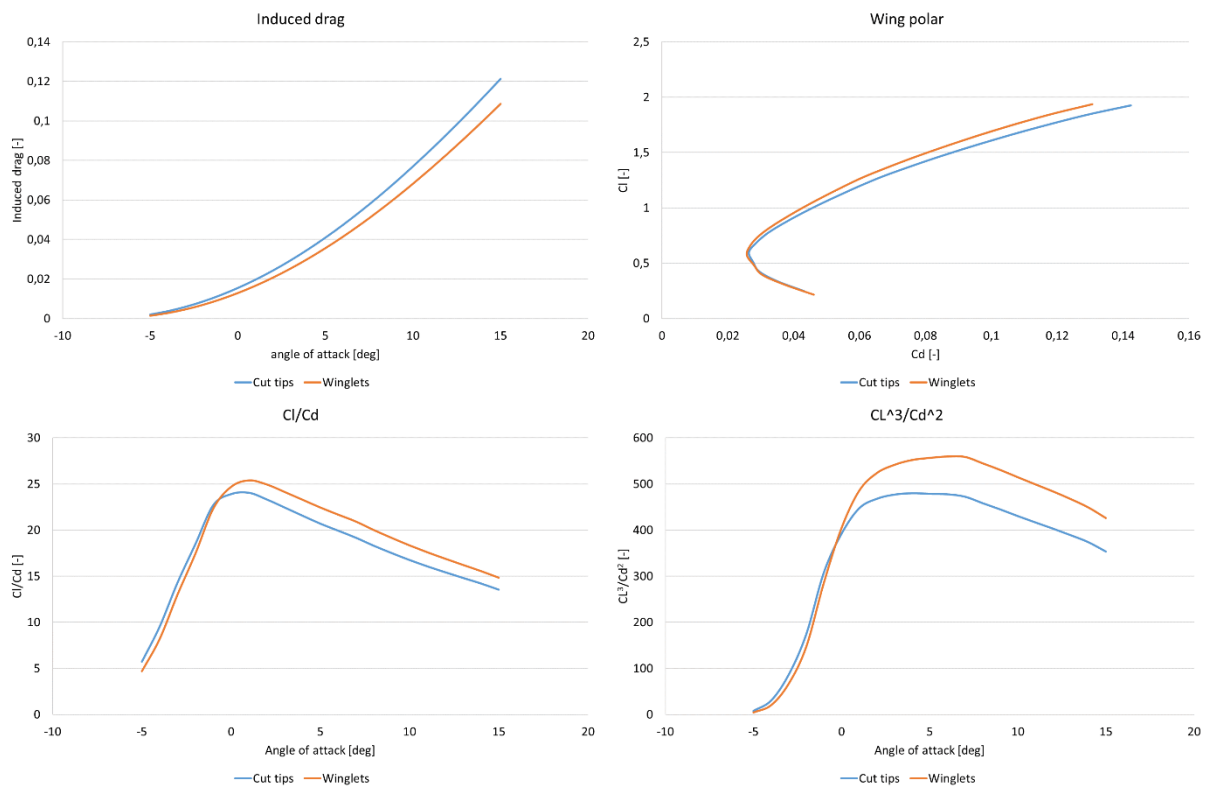


Figure 12 Winglets impact on the induced drag of the wing

6.4. Stabilator design

Due to the regulations and scoring of the ACC2022 the decision was made to make the main wing large to achieve high climb rate with the given motor and propeller setup. This meant that the greater diagonal of the rhombus was set at 2,3 m, which left little space for the stabilizer, thus a small stabilizer had to provide the plane with satisfactory control and stability. This led to the design of stabilator instead of classic horizontal stabilizer with an elevator. Another advantage of using stabilator, is that the angle of incidence isn't fixed, so it can be adjusted anytime. Due to the chosen airfoil and the large area, the main wing produced very high nose-down pitching moment. To counteract this moment the airfoil used on the stabilator is reversed NACA4412 airfoil, which produces very high pitching moment on the stabilator in order to achieve the balance of the pitching moments.

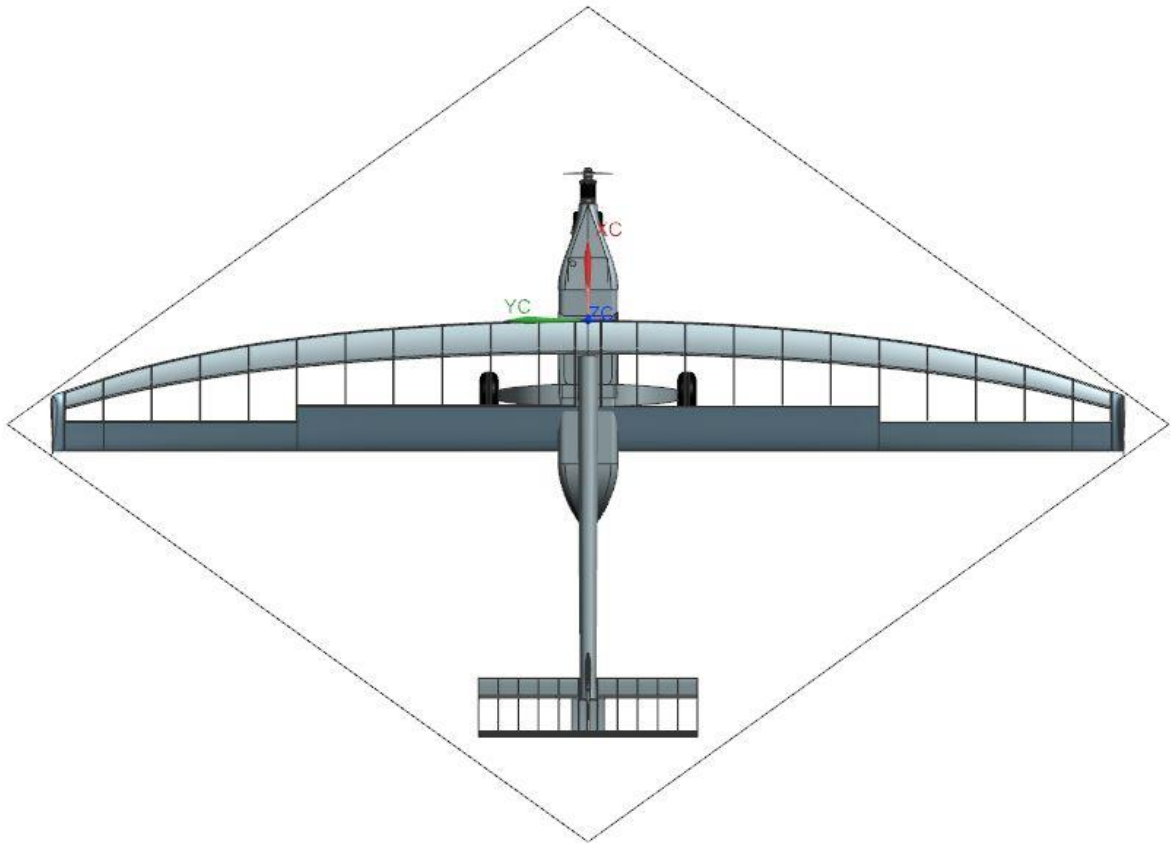


Figure 13 Plane shape inside of the rhombus box

6.5. Fin design

Aircraft's fin was designed to provide the plane with sufficient yaw control and directional stability. The airfoil of choice for the stabilizer was NACA0008 symmetrical airfoil with 8% thickness.

6.6. Servo sizing

For each of the control surfaces the calculations of hinge moments were performed using XFLR5 software along with analytical formulas. Results brought team to choose following servos.

Table 2 Servo sizing

| Control Surface | Hinge moment [Nm] | Servo |
|-------------------|-------------------|---------------|
| Aileron | 0,23 | SAVOX SW-0256 |
| Stabilator | 0,43 | SAVOX SW-0250 |
| Rudder | 0,02 | SAVOX SW-0256 |

6.7. Plane polars

After finishing the design of all of the aircraft's parts the team performed calculations of the entire plane aerodynamic properties. For the summary of the plane's aerodynamics the team chose to plot the C_l/C_d and C_m/AoA charts, as they provide information on the topic of plane's overall performance and stability.

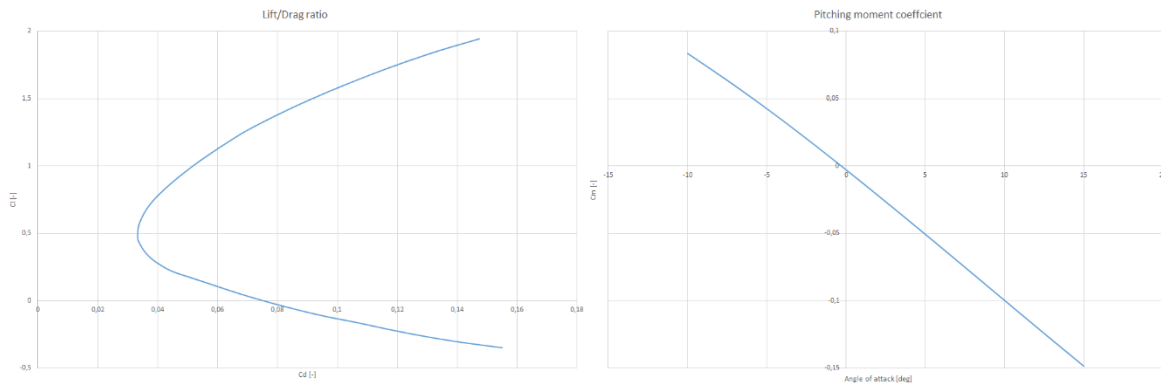


Figure 14 Plane polars

7. Stability and control

This chapter contains information on the topic of static and dynamic stability of the plane.

7.1. Mass analysis

For the forthcoming stability analysis first and foremost a mass analysis was performed to determine the position of plane's center of gravity.

Table 3 Mass analysis

| Part | mass [kg] | lever [m] | torque [Nm] |
|--------------------------------------|-----------|-----------|-------------|
| Propulsion | 0,377 | -0,098 | -0,037 |
| Automated Measuring Equipment | 0,150 | -0,125 | -0,019 |
| Battery 3s | 0,120 | 0,018 | 0,002 |
| Battery 2s | 0,048 | 0,045 | 0,002 |
| Wing | 0,530 | 0,098 | 0,052 |
| Fuselage with undercarriage | 0,955 | 0,074 | 0,071 |
| Tail boom | 0,130 | 0,550 | 0,072 |
| Fin | 0,023 | 0,720 | 0,017 |
| Stabilator | 0,040 | 0,770 | 0,031 |
| Empty mass | 2,373 | 17% MAC | |
| Payload | 3,2 | 0,123 | 0,394 |
| MTOW | 5,573 | 27% MAC | |

7.2. Static stability

The main factor used in the evaluation of the plane's stability was the calculation of neutral points of plane's horizontal stability, and further the stability margin. The desired range of the stability margin was at first set in the range of 10-15%, however during the later stages of the design process and improvements, the decision was made to aim for a smaller margin for the sake off further optimization of the horizontal stabilizer's geometry and the plane as a whole. The calculations off neutral points of stability and maneuverability were performed for the plane's MTOW and showed us that Mosquito has sufficient stability margin for all obtainable flight velocities.

Neutral points of stability and maneuverability

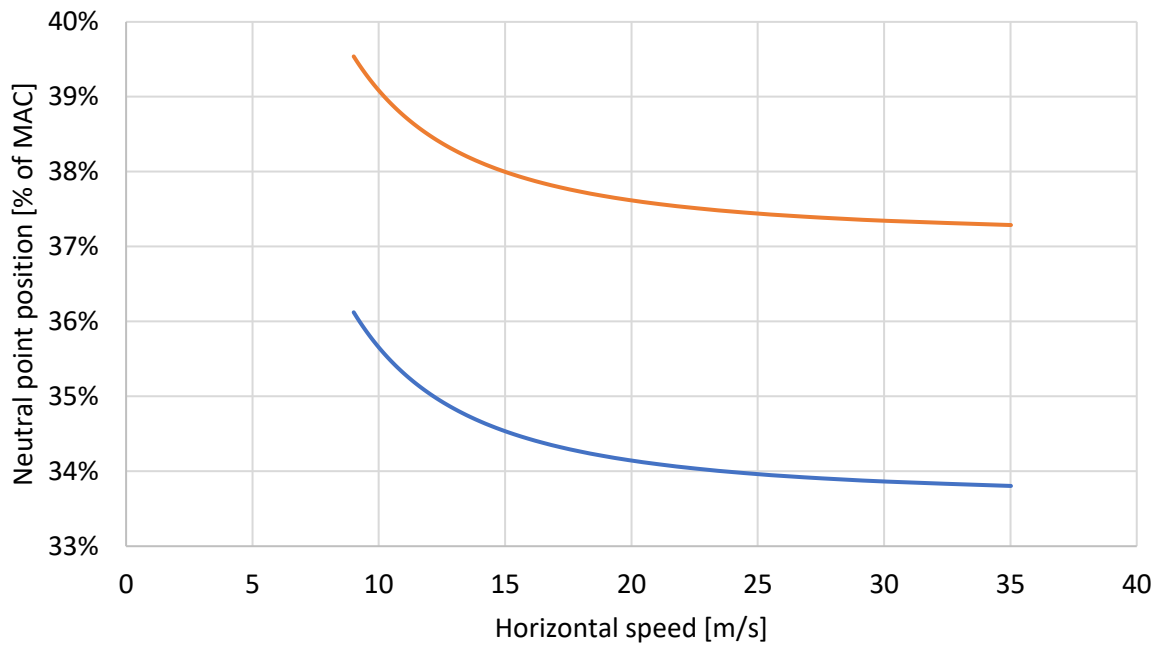


Figure 15 Neutral points of stability (blue) and maneuverability (orange) chart

For the CG situated at approximately 26% MAC stability and maneuverability margins were calculated.

Margin of stability and maneuverability

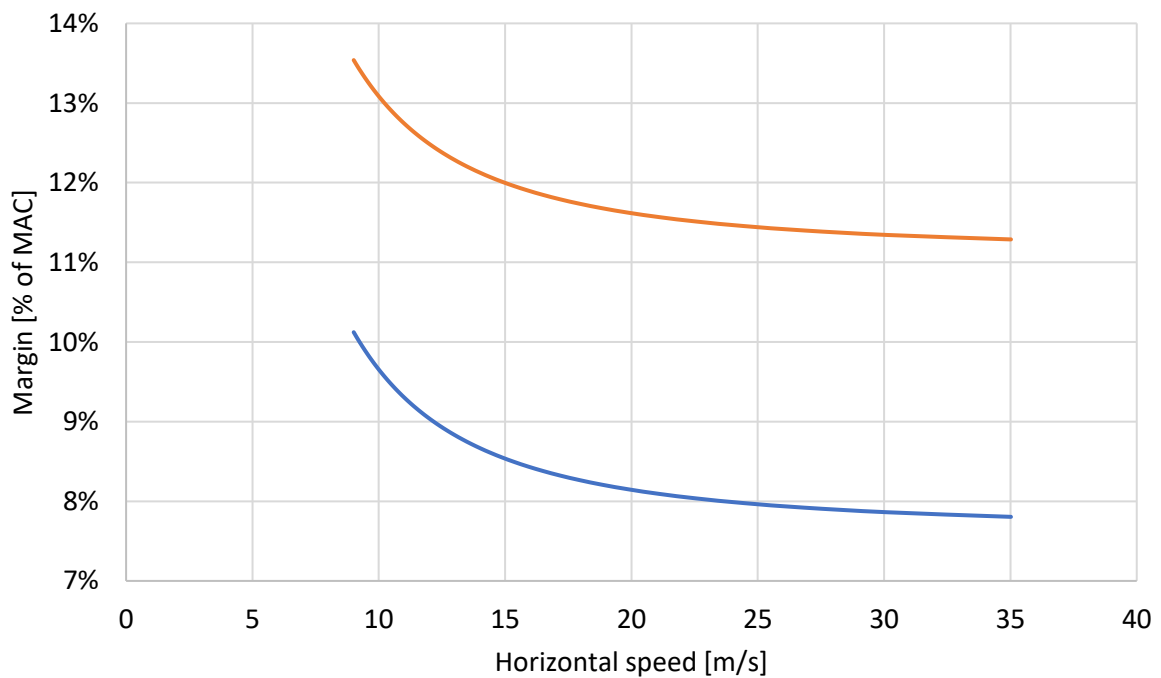


Figure 16 Margins of stability (blue) and maneuverability (orange) chart

7.3. Dynamic stability

Dynamic stability analysis was performed using XFLR5 software. The determination of the dynamic stability of the plane was based on the plane's response to different inflight instabilities. As seen in the Table 2 Mosquito is able to damp Phugoid, Roll, Dutch Roll and Short Period Oscillations, leaving only the Spiral mode not being damped by the plane itself. However, this is expected, as it is known that in order to exit the spiral mode the pilot's intervention is necessary.

Table 4 Damping coefficients

| Instability | Damping Coefficient |
|-------------|---------------------|
| SPO | -8,581 |
| Phugoid | -0,024 |
| Roll | -55,590 |
| Dutch Roll | -0,948 |
| Spiral | 0,088 |

8. Structural design

In this paragraph structural design of the aircraft's main parts is described. At the end the manufacturing process common for each part are presented.

8.1. Flight envelope

To compute loads on each part the flight envelope was elaborated. Loads from steering and wing gusts were considered. The maximum load factor equals 4,1. The flight envelope is presented on Fig. 17.

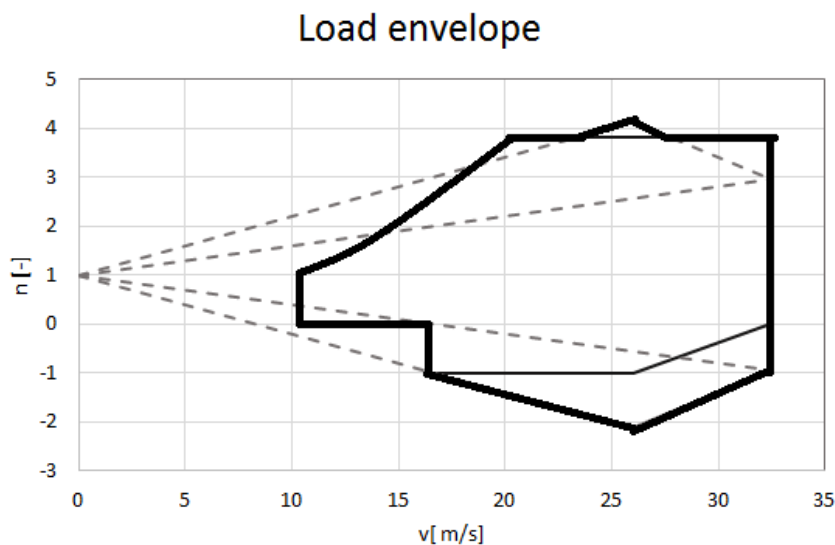


Figure 17 Flight envelope

8.2. Wing

The wing has classical single spar construction with torsion box. Strength ribs are made of carbon fiber – plywood material others are made from balsa wood. Knowing the loads the C-shape spar and torsion box were analyzed. Bending and twisting moment are presented on Fig. 18. Due to lack of low density carbon fiber, the team decided to make carbon spar and fiber glass torsion box.

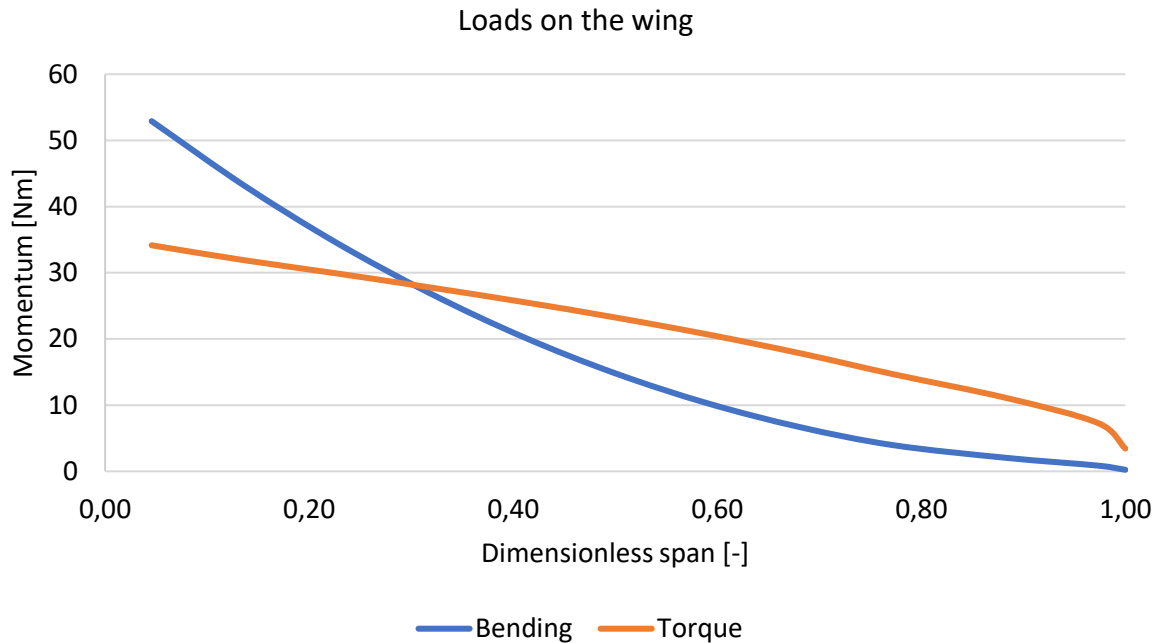


Figure 18 Wing loads chart

The separate composite parts are made on molders, then assembled on polymethyl fixers. The torsion box is made of two separate parts glued together in one process with internal ribs and spar. After that other external parts of the wing were glued.

On the figures below manufacturing process of prototype parts is shown.

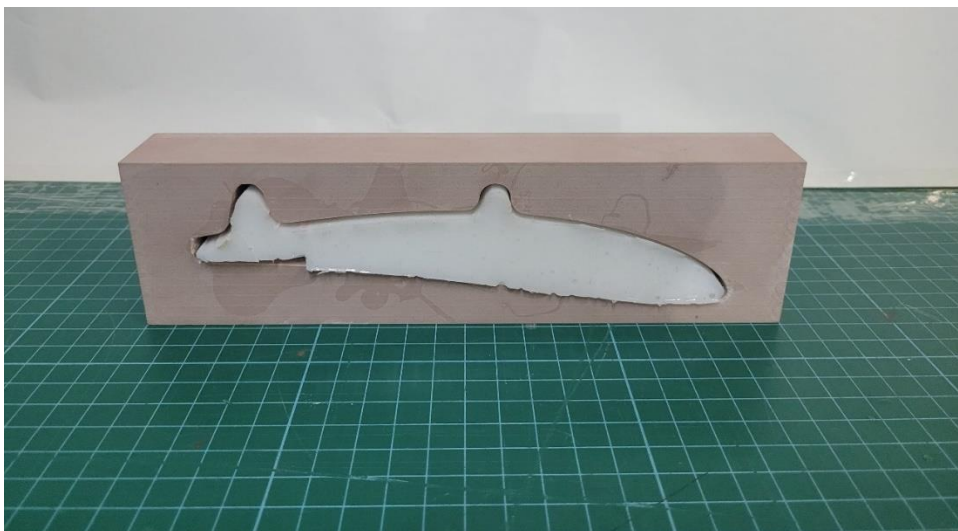


Figure 19 Mounting rib molder with gumosil negative

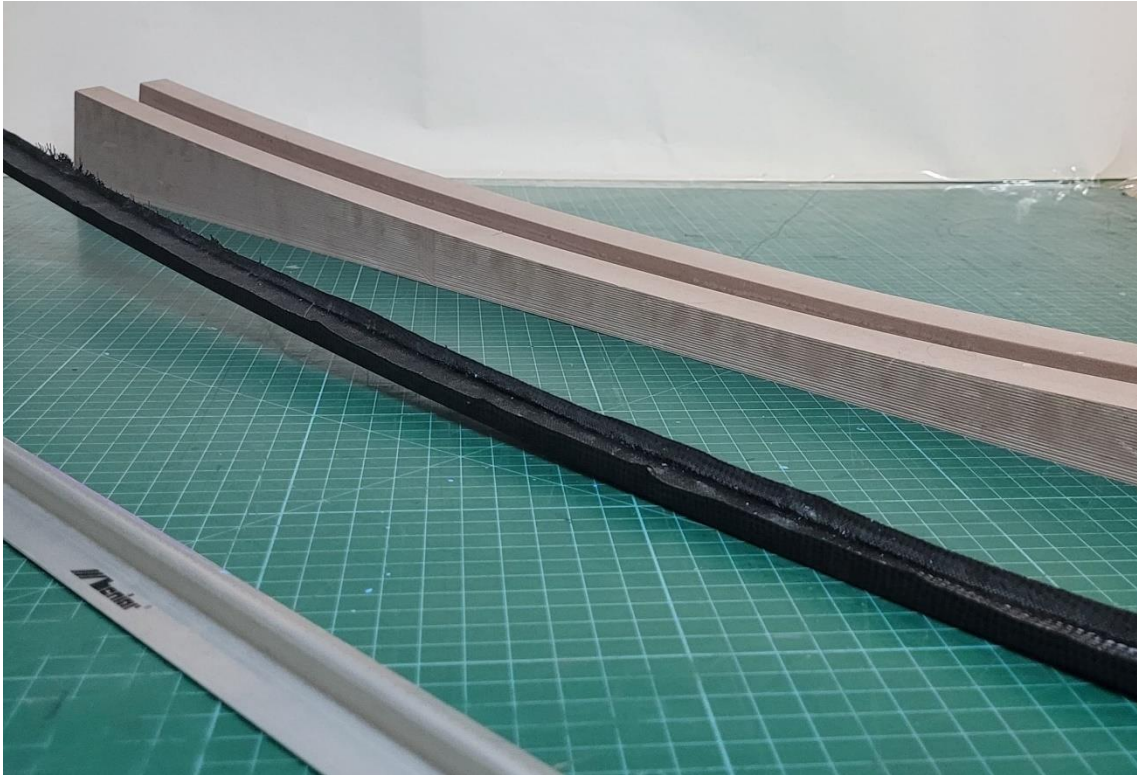


Figure 20 Wing spar with molder

8.3. Winglets

Winglets and blends are made of polystyrene core with carbon fiber spars covered with fiberglass to achieve high smoothness of surface. Trailing edges are also made of polystyrene but covered with aluminum foil to achieve higher stiffness.

8.4. Stabilator

Stabilator's structure consists of single balsa box spar with balsa torsion box. Ribs are made out of balsa wood with plywood or balsa-plywood strength ribs. On the leading and trailing edges there are balsa boards which help with the integration of the structure as well as add stiffness to the structure. Due to the small loads on the stabilator a decision was made to cover the structure with just heat-shrinkable foil. The whole structure is integrated on polymethyl fixers. To allow the whole structure to rotate, there are aluminum tubes embedded into the spar, which acts as a hinge axis for the stabilator. The tubes go through the tail boom and mounts glued to the surface of the tail boom. The decision was made to make a wooden structure instead of polystyrene, as such structure should result in smaller stabilator's weight.

8.5. Fin

Fin is designed with a simple structure containing balsa box spar with balsa ribs. On the leading edge balsa board is mounted to add stiffness and help with the fin's integration. The 4th rib is reinforced in order to mount a rudder servo on it. The rudder is milled from polystyrene. The whole structure is covered with the heat-shrinkable foil.

8.6. Fuselage and cargo bay

Fuselage is made of both carbon fiber and fiber glass with Herex mid-layers to prevent surface buckling. The fuselage has a plywood frame. Such construction allows to manufacture lightweight stiff fuselage to which all propulsion and payload will be attached.

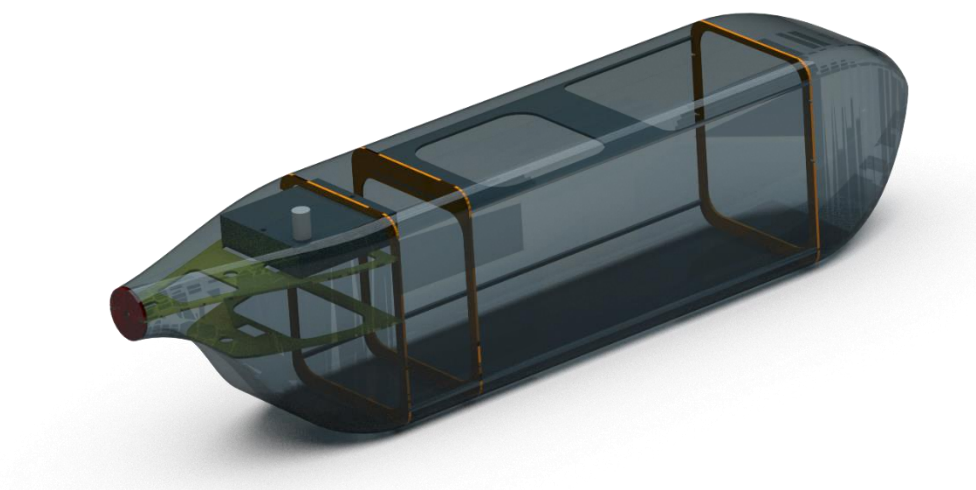


Figure 21 Fuselage design

During initial design three configurations were considered for the cargo bay accommodation: loading from aft using special drawer, loading from aft separate bags and loading from side separate bags, shown on the Fig. 22 in their respective order.

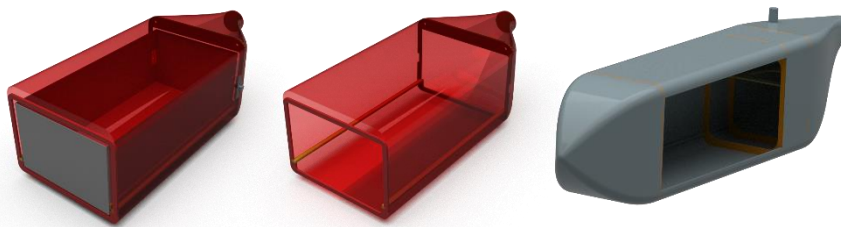


Figure 22 Cargo bay accommodations

The team chose to load and unload cargo from one side of the aircraft. Such configuration allows easy access to every bag. The measuring equipment is located at the top of the frontal part of the fuselage, which is covered with glass fiber.

8.7. Tail boom

Tail boom design began with strength analysis. The shape of the tail boom is restricted by the shape of cone core on which the parts are manufactured. The performed calculations based on analytical formulas allowed us to compute the movement of the tail boom tip. The shape of deflection and manufacturing process is presented on the Fig. 23 below. The tail boom has composite structure with balsa wood mid layer. The mass of the part is approximately 130g.



Figure 23 Tail boom displacement chart and measurement method

8.8. Landing gear

Main landing gear is made of carbon fiber composite with balsa core. The team has decided to build at least 2 different struts, one with increased stiffness. Such redundancy allows us to choose the optimal gear for grass runway.

Front landing gear has two wheels to minimize friction. Track width provides higher stability in case of potholes. The front strut has its own suspension. The selection of wheels for the rear part of gear was based on sliding and rolling friction tests. They were carried out under the most suboptimal weather conditions possible at the place where competition take place. A test platform in the form of a fuselage from another aircraft was used for the tests. As a result, Kavan Superlight 100mm wheels were chosen, which stand out with low rolling resistance and high ability to absorb energy.

Landing gear is steerable.



Figure 24 Landing gear test platform

8.9. Structural division

The Mosquito aircraft is built from 9 major parts: fuselage, left and right wing, tail boom with stabilator, vertical stabilizer, main landing gear strut and winglets. Such structural division makes it easy to transport in cargo box. To unload the aircraft it is recommended to use table, however it is not mandatory.

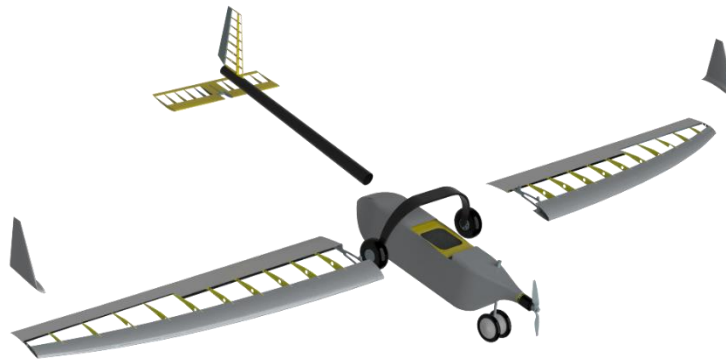


Figure 25 Aircraft structural division

9. Performance

This chapter contains information on the topic of plane's performance, specifically on the parameters that would be taken into account during the calculation of the aircraft's score, such as climb rate, horizontal speed, payload and turn.

9.1. Climb rate and horizontal speed

Due to the regulations of the competition, our team has been given the challenging task of designing a plane that performs well in different areas, so we had to pick some starting point during the process. The decision was made that climb rate would be an ideal parameter as its scoring is the most predictable out of all scoring tasks, thus our goal was to achieve maximum score for achieved altitude. Considering the 60 second given for the climb, take-off time and safety factor, our team set the goal to achieve a minimal climb rate of 1,8 m/s, to reach the 100m altitude. As seen on the Fig 26 plane's maximum climb rate is higher than assumed speed of 2 m/s, which leaves us with satisfactory safety factor in case the actual performance was weaker than calculated values.

Horizontal speed was off secondary importance, as the scoring for this task was highly dependent on the performance of other competing teams. However, all possible measures were taken as to achieve the lowest attainable drag, such as designing winglets, resulting in the increase of the vertical speed of the plane.

The calculations provided us with the following vertical and horizontal speed chart.

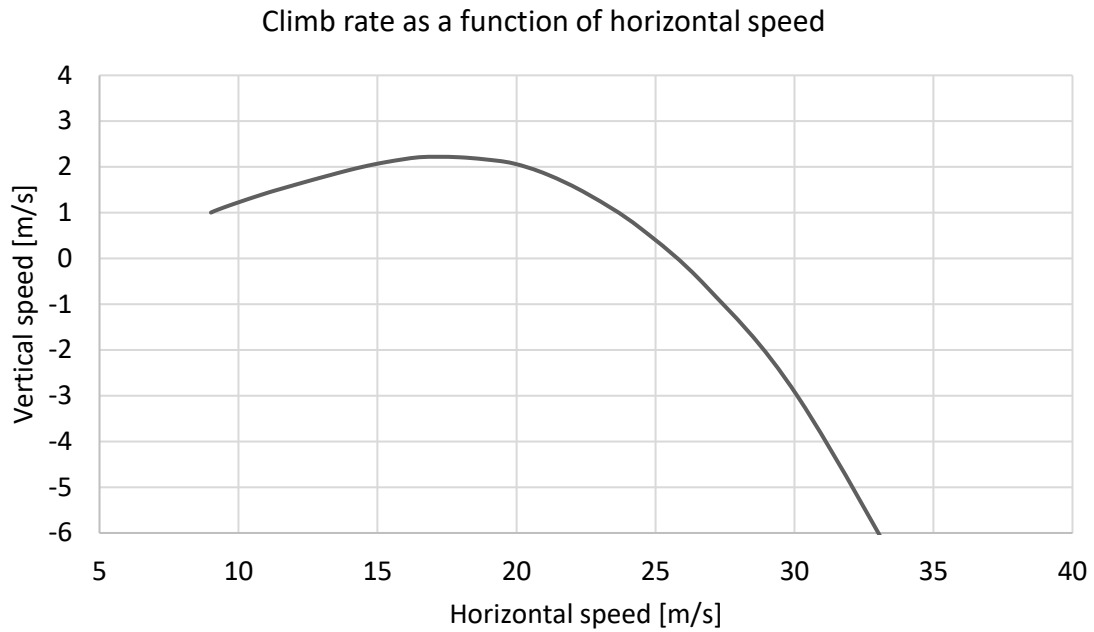


Figure 26 Climb rate chart

9.2. Turn analysis

Due to the size restrictions of the airfield our team performed an analysis of the turn radius in order to determine whether our aircraft is able to turn within the area of airfield, the cruise speed of the plane is also shown on the chart below to make the determination easier. Looking at the picture of the airfield as shown in the regulations the smallest circle that is tangent to its top and bottom lines has a diameter of approximately 180 m, which is also shown on the chart below. This means, that for all the bank angles, other than 10° and 20° and granted that plane is flying at its cruise speed, which is around 26 m/s, there shouldn't be a problem to make a turn within the said smallest circle. Furthermore, assuming that the chosen trajectory is not using the narrowest part of the airfield, with the broadest part having more than 250m, the turn with the bank angle of 20° and cruise speed should also be possible.

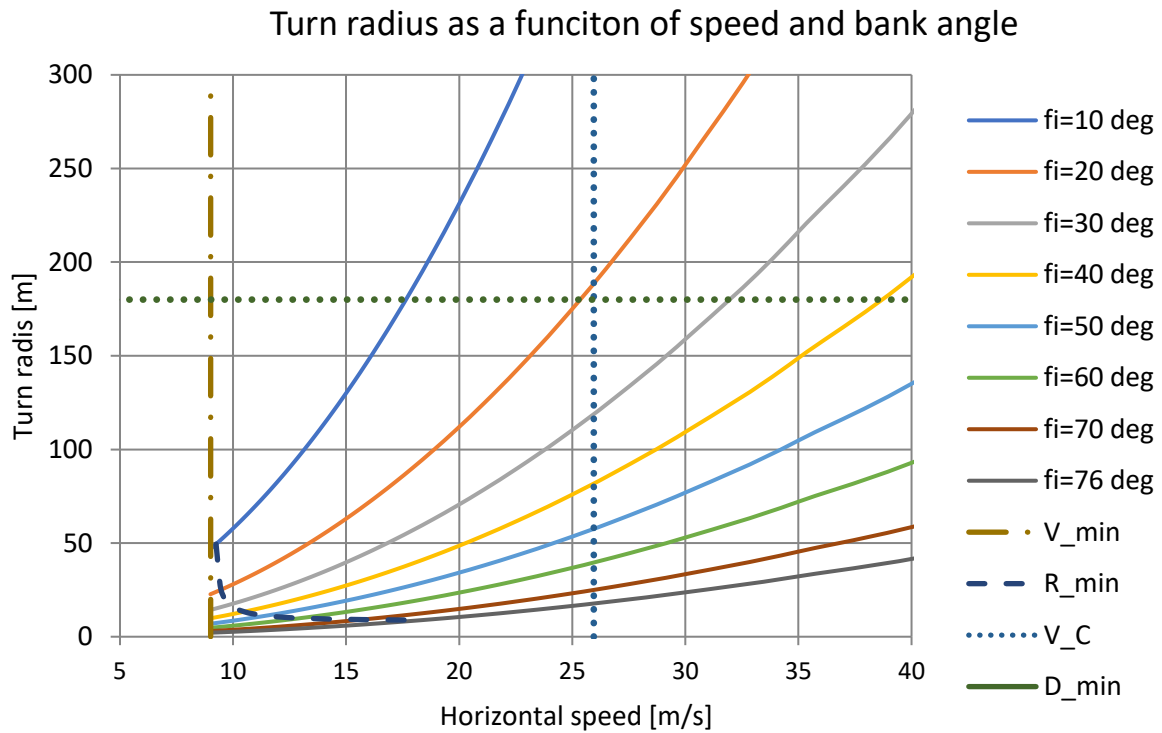


Figure 27 Turn radius analysis with the cruise speed VC (blue dotted line) and smallest diameter of the airfield (dark green dotted line)

9.3. Take-off run analysis

During the design process the take-off run length was calculated. In order to minimize calculation methods, test flights were performed. The team used one of our old aircrafts for which the calculations were performed. It turned out that applied formulas had error of about 20%. It is noticeable that the take-off run length depends almost linearly on the mass of the aircraft.

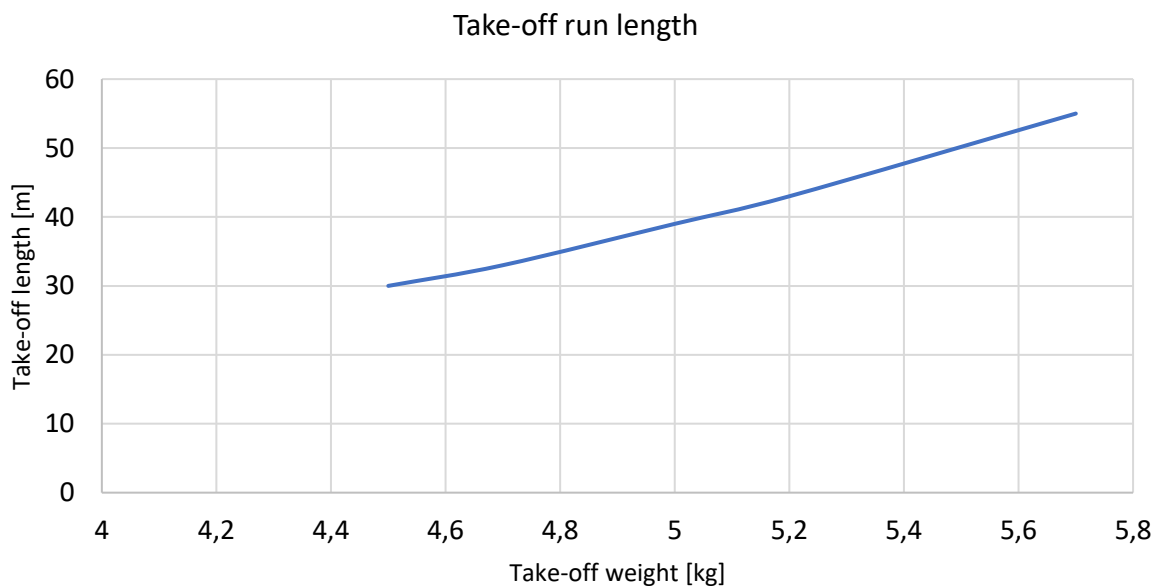


Figure 28 Take-off length chart

9.4. Representative properties

For the summary of plane's performance the team chose few specific parameters which showcased the best how Mosquito performs. The maximal climb rate is considerably higher than the assumed value, such safety factor was considered advisable as the climb rate time measurement starts upon reaching the velocity of 5 km/h by the GPS module, and viscous drag is undermined by the panel method, so reaching higher analytical climb rate is beneficial.

Table 5 Performance summary

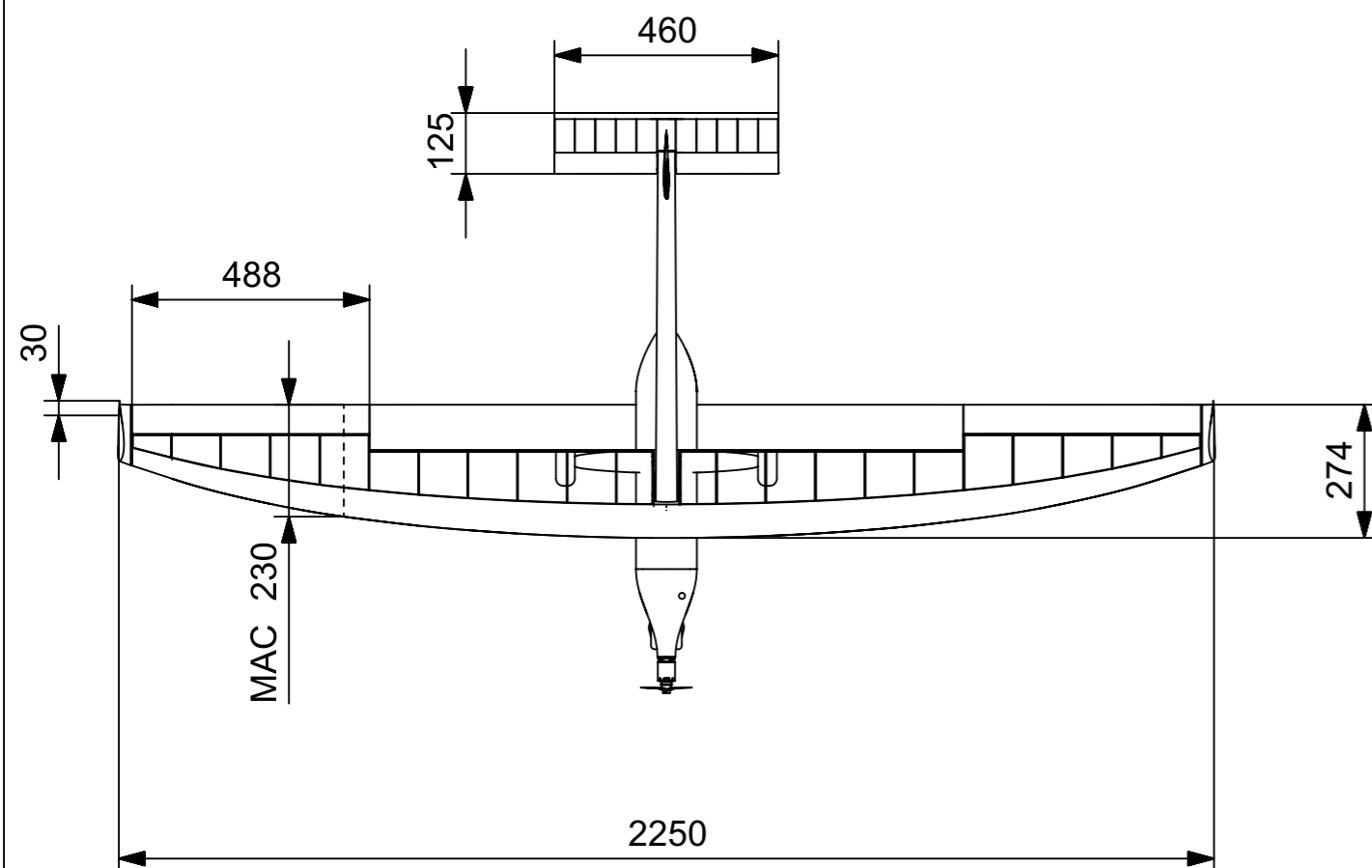
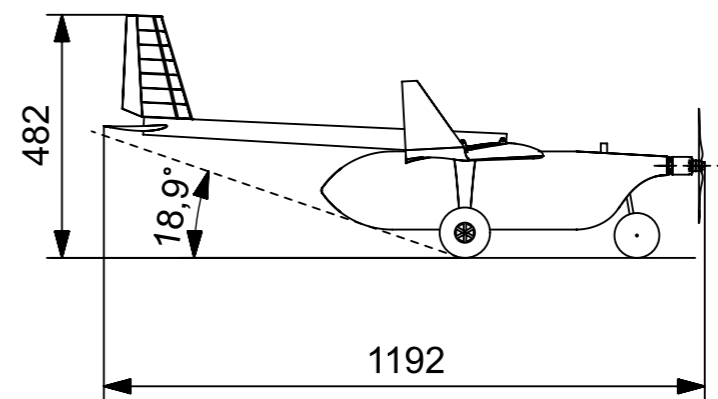
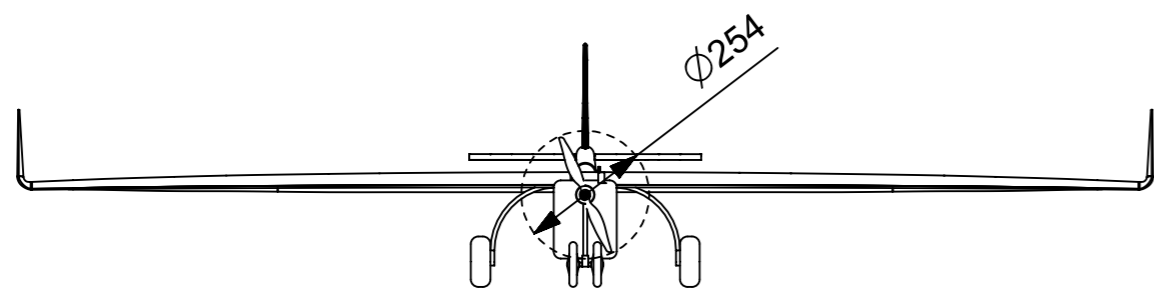
| n_{\max} | V_s | V_c | V_D | w_{\max} | m_{payload} |
|------------|--------|--------|--------|------------|----------------------|
| +4,1 | 10 m/s | 26 m/s | 32 m/s | 2,1 m/s | 3,2 kg |

10. Outlook


This is the first time our club would participate in Air Cargo Challenge competition, as previously our club was focused on the SAE Aero Design competition exclusively. With ACC 2022 our target was to design an aircraft which would allow us to compete with the other teams.

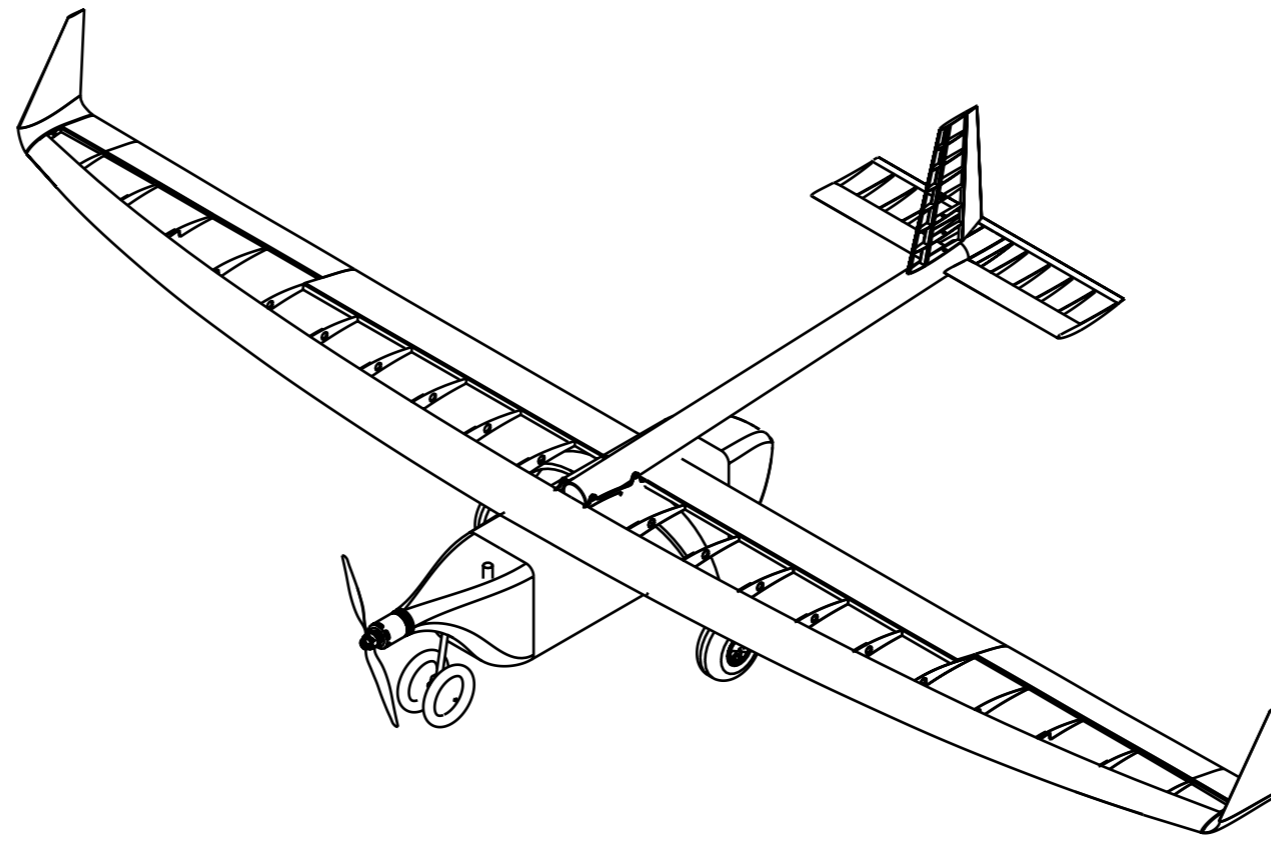
This year's rules turned out to be quite demanding for our team, as the aircraft described by the rules should excel in many different areas, but we took it as an opportunity to face a completely new challenge.


The presented construction fulfils our assumptions and predictions made during the early stages of the design process. We hope that Mosquito will be able to accomplish its mission and allow our team to finish the competition with good results.

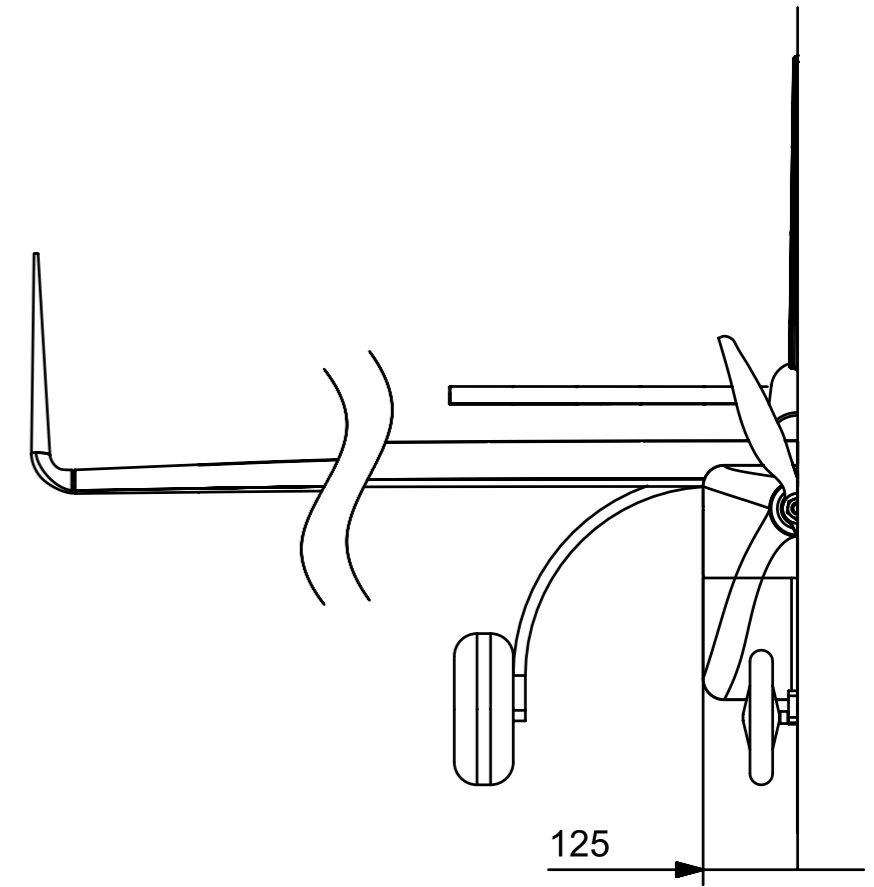
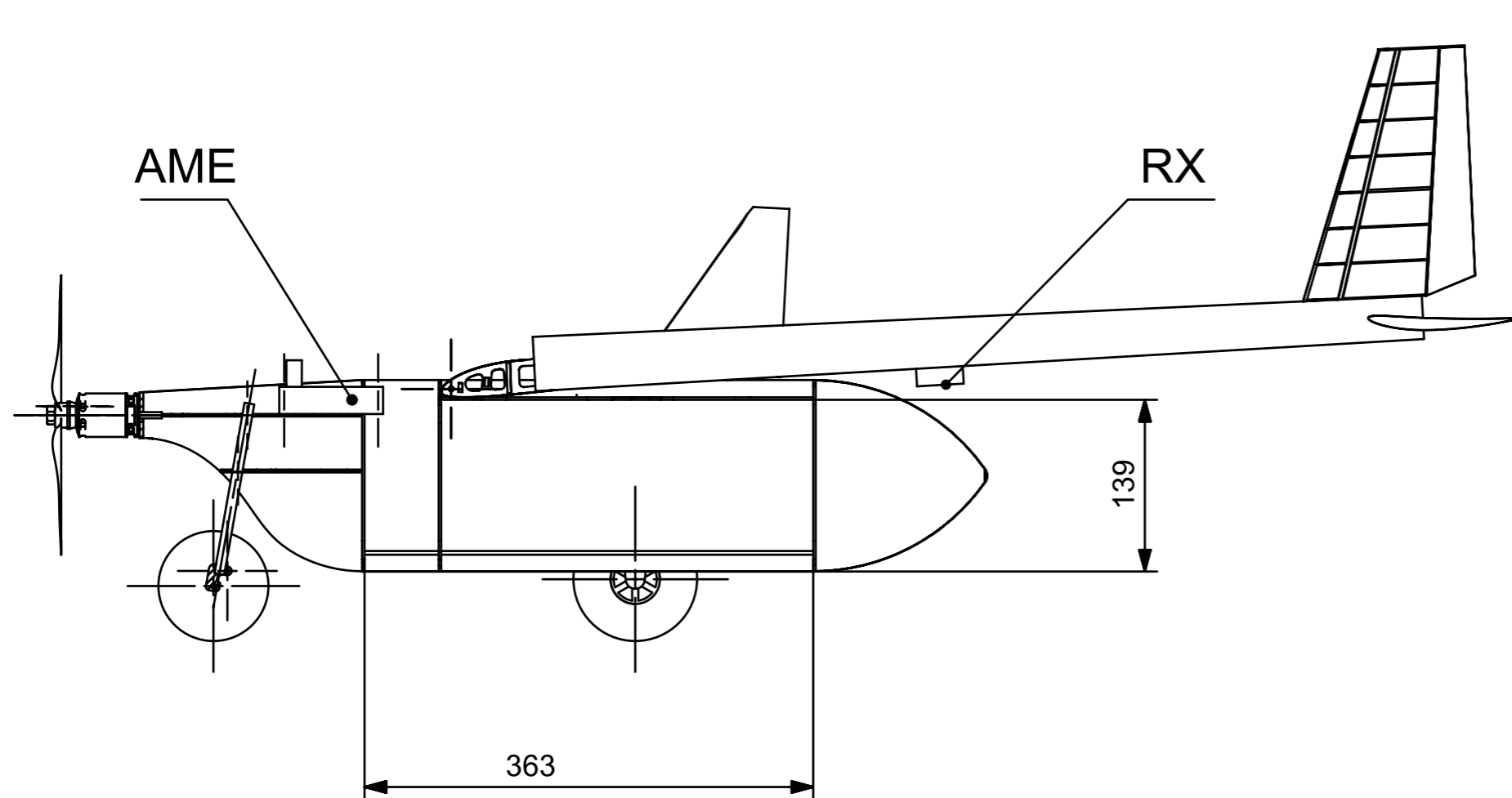



| | |
|------------|---|
| Wing | Airfoil: PP02 10% thickness Area: 0.5m ² Span: 2250m MAC: 230mm Aspect ratio: 10 |
| Fuselage | Length: 685mm With: 125mm Cubature of payload bay: 0.007m ³ Front area: 0.0192m ² |
| Stabilator | Airfoil: NACA4408 (reversed) Area: 0.0575m ² Span: 460mm Cord: 125mm Aspect ratio: 3.7 Volume: 0.30 |
| Fin | Airfoil: NACA008 Area: 0.023m ² Height: 230mm MAC: 104mm Volume: 0.015 |

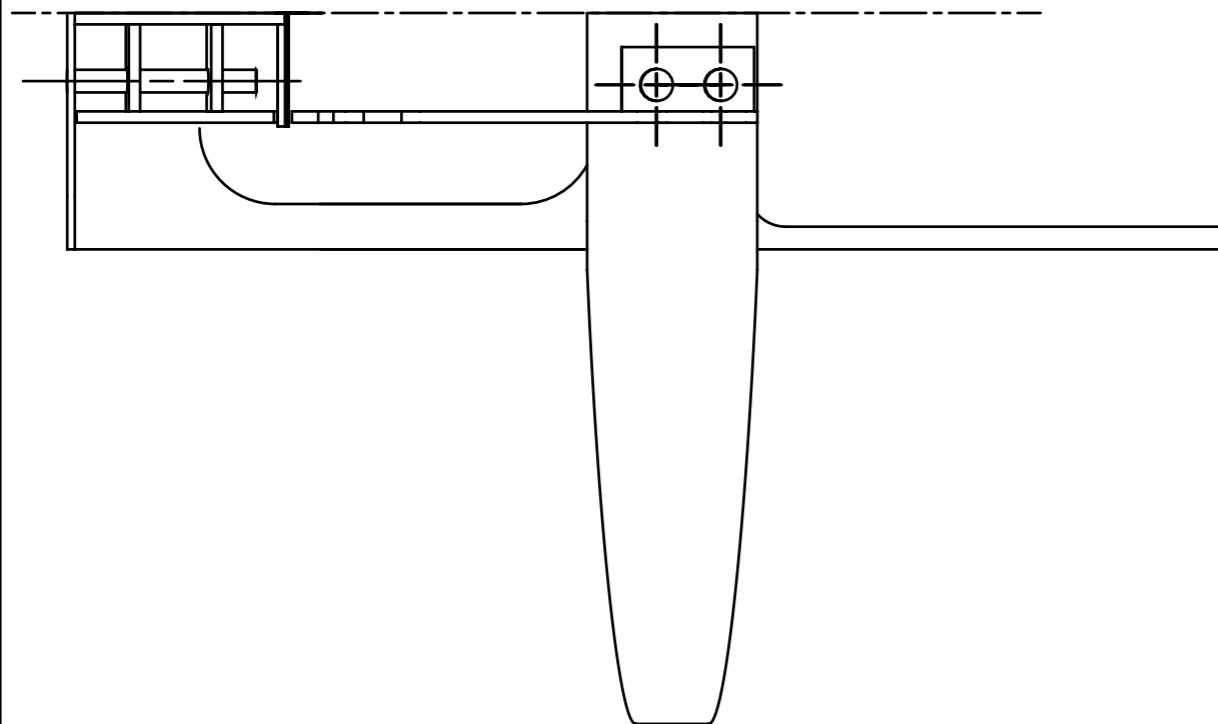
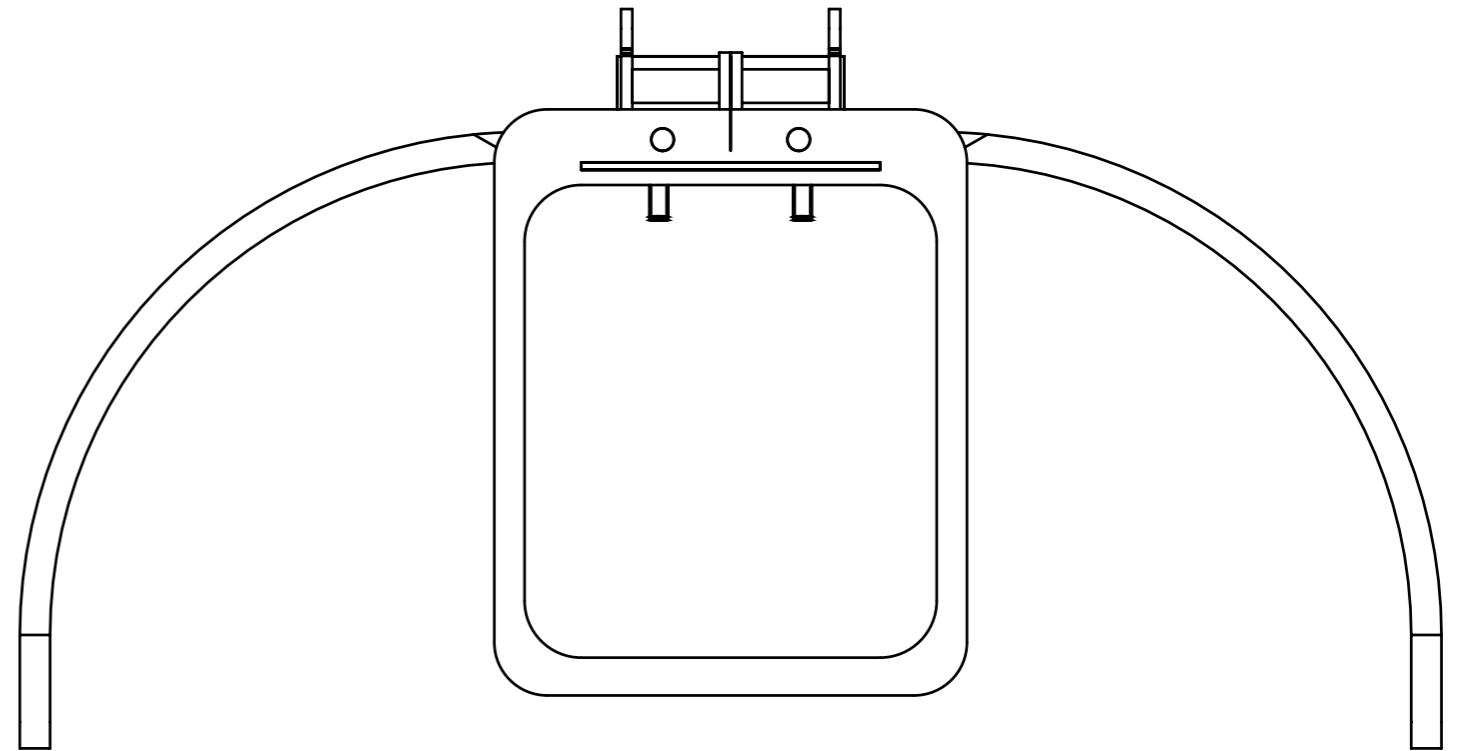
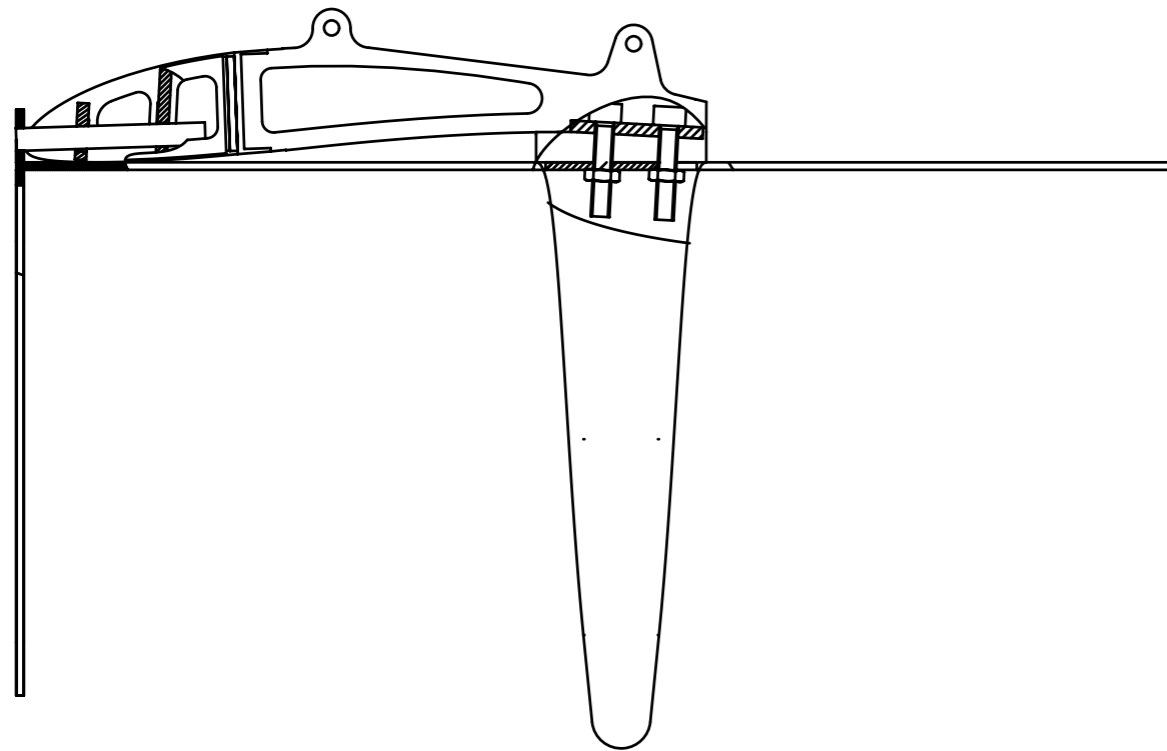
| | | | |
|---------------------------------|---|----------|-------------------------------------|
| Format A3 |  | Drawn | G. Muchla 2022.05.27 |
| | | Designed | G. Muchla K. Wojtacki 2022.05.27 |
| | | Scale | 1:15 |
| | WUT AeroDesign | 29 | |
| Warsaw University of Technology | Name | Mosquito | Number |
| | | | Attachment 1 |
| | | | 1/1 |




| | | | | | |
|------------------------------------|---|----------------------------|-----------|-------------------------------------|--------------|
| Format A3 |  | | Drawn | G. Muchla 2022.05.27 | |
| | | | Designed | G. Muchla K. Wojtacki 2022.05.27 | |
| | | | Podzialka | 1:10 | |
| | WUT AeroDesign | 29 | | | |
| Warsaw University of Technology | Name | Isometric view Mosquito | | Number | Attachment 2 |
| | | | | | 1/1 |



| | | | | |
|------------------------------------|---|----------|----------|-------------------------------------|
| Format A3 |  | | Drawn | G. Muchla 2022.05.28 |
| | | | Designed | G. Muchla K. Wojtacki 2022.05.28 |
| | | | Scale | 1:5 |
| | WUT AeroDesign | 29 | | |
| Warsaw Univeristy of Technology | Name | Fuselage | Number | Attachment 3 |
| | | | | 1/1 |



| | | | | | | |
|------------------------------------|---|------------|----------|-------------------------------------|--------------|-----|
| Format A3 |  | | Drawn | G. Muchla 2022.05.28 | | |
| | | | Designed | G. Muchla K. Wojtacki 2022.05.28 | | |
| | | | Scale | 1:2 | | |
| | WUT AeroDesign | 29 | | | | |
| Warsaw University of Technology | Name | Wing mount | | Number | Attachment 4 | |
| | | | | | | 1/1 |